

Eley–Rideal and Langmuir–Hinshelwood Recombination Coefficients for Oxygen on Silica Surfaces

M. Cacciatore* and M. Rutigliano†

University of Bari, 70126 Bari, Italy

and

G. D. Billing‡

University of Copenhagen, DK 2100 Copenhagen, Denmark

The energetics and dynamics of the Eley–Rideal (E–R) and Langmuir–Hinshelwood (L–H) recombination reaction of oxygen atoms on β cristobalite have been studied within a semiclassical collisional model. The calculated recombination coefficient γ for the E–R reaction at $T_s = 1000$ K is in satisfactory agreement with the experimental value, whereas at $T_s = 600$ K a satisfactory agreement is found between the L–H γ value and the experimental one. Results on the energy exchanges between the formed O_2 molecules and the silica surface are reported. Site-specific effects as well as the influence of the top layer surface structure are also pointed out and discussed.

Nomenclature

E_{kin}	= kinetic energy
E_{rot}	= rotational energy
E_{tr}	= translational energy
E_{vib}	= vibrational energy
e	= charge unit
H_{eff}	= effective Hamiltonian of the atom/surface system
h	= Planck constant
j	= rotational quantum number
K	= Boltzmann constant
m_i	= mass of particle i
N	= total number of surface atoms
$P_{\text{E–R}}$	= E–R recombination probability
$P_{i\gamma}$	= γ component of the momentum of particle i
P_r	= recombination probability
Q_k	= normal coordinate of phonon mode k
R_i	= position coordinates of gas particle i
$R_{i\alpha}^{\text{eq}}$	= equilibrium distance between gas-phase atom i and lattice atom α
$R_{\text{O–O}}$	= intramolecular distance of O_2
$R(t)$	= classical trajectory of gas particles
r_{in}	= distance between gas atom i and lattice atom n
T_s	= surface temperature
$T_{\alpha j, k}$	= transformation matrix between coordinates $\eta_{\alpha\gamma}$ and Q_k
t	= time
V_C	= coulomb potential
V_{eff}	= effective potential
V_{int}	= gas/surface interaction potential
$V_k^{(1)}$	= first derivative of the interaction potential with respect to the k th normal mode coordinate Q_k
V_{O_2}	= interatomic potential of O_2

V_0	= interaction potential between the gas-phase particles and the lattice atoms in the equilibrium position
ν	= vibrational quantum number
$X_{\alpha\gamma}$	= γ component of the Cartesian coordinate of lattice atom α
Z_n	= charge of lattice atom n
γ	= recombination coefficient
ΔE_{exo}	= reaction exothermicity
ΔE_k^{\pm}	= energy loss(+) / gained(–) with the phonons
ΔE_{ph}	= energy exchanged with the phonons
δ_{\pm}	= quadrupole charge of molecular oxygen
η_k	= phonon excitation strength of phonon mode k
$\eta_{\alpha\gamma}$	= γ component of the mass-weighted coordinates of atom α
ρ_k	= excitation probability of phonon mode k
τ	= time unit
ω_k	= frequency of phonon mode k

Subscripts

ad	= adsorbed
eff	= effective
eq	= equilibrium
exo	= exothermic
exp	= experimental
gas	= gaseous
int	= interaction
ph	= phonon

I. Introduction

RECENTLY, the oxygen atom recombination on silica-based surfaces has attracted considerable interest because of the importance of this reaction in the spacecraft thermal protection problem for some NASA and future European shuttle re-entry missions.¹ The recombination reaction is, in fact, exothermic, so that part of its exothermicity can appear as excitation of the internal degrees of freedom of the formed O_2 molecules, whereas the energy excess can be transferred as heat to the surface substrate. Despite the great deal of experimental work,^{1–5} some uncertainty exists on the recombination coefficient γ of oxygen (and nitrogen) atoms on silica, so that the actual catalytic activity of such surfaces and a precise understanding of the atom recombination processes seems to not be completely achieved.

On the theoretical side, very few studies on this subject have appeared in the literature. The kinetics of the oxygen and ni-

Received June 8, 1998; presented as Paper 98-2843 at the AIAA/ASME 7th Joint Thermophysics and Heat Transfer Conference, Albuquerque, NM, June 15–18, 1998; revision received Oct. 21, 1998; accepted for publication Oct. 21, 1998. Copyright © 1999 by the American Institute of Aeronautics and Astronautics, Inc. All rights reserved.

*Research Director, CNR–Centro di Studio Chimica dei Plasmi, Dipartimento di Chimica via Orabona N°4. Member AIAA.

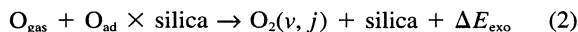
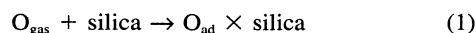
†Graduate Student, CNR–Centro di Studio Chimica dei Plasmi, Dipartimento di Chimica via Orabona N°4.

‡Full Professor, Department of Chemistry, H. C. Ørsted Institute.

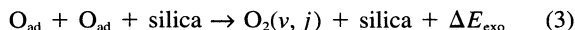
trogen atom recombination on silica have been investigated by Jumper and Seward,⁶ Nasuti et al.,⁷ and Gordietz et al.,⁸ by solving the properly defined parametric steady-state rate equations.

On the other hand, molecular dynamic studies on this system are practically absent. Molecular dynamic calculations have been, in fact, carried out for only a very limited number of recombination reactions, among which are the CO formation on Pt surfaces⁹⁻¹¹ and hydrogen atom recombination on metallic substrates.¹²⁻¹⁶ The results obtained in these studies have been very helpful in getting a better understanding of the different behaviors of the recombination process that cannot be pointed out within a classical kinetic approach, such as the total energy partitioning and the energy loss to the surface. The present study is a first attempt to describe the dynamics of oxygen recombination on silica.

Atom recombination reactions are usually described according to two extreme collisional mechanisms: the Eley-Rideal (E-R) mechanism,



and the Langmuir-Hinshelwood (L-H) mechanism,



The E-R reaction is a two-step process: first an oxygen atom is chemisorbed, then the reaction occurs between the adatom and the oxygen approaching the surface from the gas-phase. In the L-H mechanism, the reaction takes place between two adsorbed atoms that propagate on the surface and then eventually recombine. In this study, both the E-R and L-H reactions are investigated.

We describe the dynamics of the oxygen atoms in the gas phase and the dynamics of the lattice atoms according to the semiclassical collisional method that has been developed and successfully applied for the description of several reactive surface processes.^{9,10,14-16} In the model, the most important features of the recombination reaction are described and incorporated in the simulation at a reasonable level of accuracy. The results of the investigation are presented and discussed, referring to the recombination probabilities, energy deposited to the surface, and internal energy distributions in the formed O₂ molecules. In addition to this, two important aspects in the catalytic reactions are also considered and investigated, namely, the effect of the top layer surface structure and the effect of the different adsorption sites on the recombination dynamics.

II. Semiclassical Dynamical Calculations

The assumed collisional model is semiclassical in the sense that the dynamics of the gas-phase oxygen atoms are described classically, whereas the lattice phonons are quantized. The dynamical coupling between the surface vibrations and the oxygen atoms is described by solving the classical Hamilton's equations of motion for the translational degree of freedom of the oxygen atoms in an effective Hamiltonian H_{eff} :

$$\frac{dR_i}{dt} = \frac{P_{Ri}}{m_i}, \quad \frac{dP_{Ri}}{dt} = -\frac{dH_{\text{eff}}}{dR_i} \quad (4)$$

where H_{eff} is defined as

$$H_{\text{eff}} = \frac{1}{2} \sum_{i,y} \frac{1}{m_i} P_{iy}^2 + V_{\text{O}_2}(R_{\text{O-O}}) + \Delta E_{\text{ph}} + V_{\text{eff}} \quad (5)$$

V_{O_2} and ΔE_{ph} are, respectively, the intramolecular O₂ potential and the energy exchanged with the silica surface. Accord-

ing to the Ehrenfest theorem, we define the effective potential, V_{eff} , as the expectation value of the interaction potential V_{int} over the total phonon wave function: $V_{\text{eff}}(t, T_s) = \langle \Psi_{\text{ph}} | V_{\text{int}} | \Psi_{\text{ph}} \rangle$. The time evolution of $|\Psi_{\text{ph}}(t)\rangle$ for the phonon states is obtained by solving the time-dependent Schrödinger equations for a set of $(3N-6)$ independent harmonic oscillators (N being the total number of atoms in the lattice) perturbed by the external forces exerted between the atom/molecule in the gas phase and the solid substrate. We further expand the interaction potential V_{int} up to the first term of Q_k :

$$V_{\text{int}} = V_0 + \sum_k V_k^{(1)} Q_k \quad (6)$$

where V_0 is the static potential between the atoms in the gas phase and the lattice atoms in their equilibrium positions, and $V_k^{(1)}$ is the first derivative of V_{int} with respect to Q_k , with Q_k being the normal mode coordinate of the k th phonon mode. These derivatives can be evaluated by using the relation between the mass-weighted coordinates of the lattice atoms, $\eta_{\alpha\gamma} = (X_{\alpha\gamma} - X_{\alpha\gamma}^{\text{eq}})/\sqrt{m_{\alpha}}$, and Q_k :

$$V_k^{(1)} = -\frac{1}{2} \sum_{i,\alpha} \frac{1}{\sqrt{m_{\alpha}}} \frac{1}{R_{i\alpha}^{\text{eq}}} \frac{\partial V_i}{\partial R_{i\alpha}} \bigg|_{\text{eq}} \sum_j T_{\alpha j,k} (X_{\alpha j} - X_{\alpha j}^{\text{eq}}) \quad (7)$$

Using Eq. (6), an analytical solution of the quantum equations of motion for the lattice vibrations is possible, and the following expression for V_{eff} is obtained^{9,10,17}:

$$V_{\text{eff}}(t, T_s) = V_0 + \sum_k V_k^{(1)} \eta_k(t) \quad (8)$$

where $\eta_k(t)$ are the phonon excitation strengths, given in terms of the Fourier components of the external forces $I_{i,k}(t)$:

$$\eta_k(t) = -\int dt' (\hbar \omega_k)^{-1} \frac{d}{d\rho_k} (\Delta E_k^+ + \Delta E_k^-) \times \{I_{c,k}(t') \cos[\Theta_k(t')] + I_{s,k}(t') \sin[\Theta_k(t')]\} \quad (9)$$

$$I_{c,k} = \int_{-\infty}^{+\infty} dt V_k^{(1)} [R(t)] \cos(\omega_k t) \quad (10)$$

where $\Theta_k(t) \sim \omega_k t$, ω_k is the frequency of the k th phonon mode, whereas $\Delta E_k^{\pm} = \Delta E_k^{\pm}(\omega_k, \rho_k^{\pm}; T_s)$ is the energy loss(+) / gained(-) of the chemical species as a result of the phonon excitation (+) and de-excitation (-) processes in the k th vibrational normal mode of the silica substrate.^{9,10,14} The total energy exchanged between the chemical species and the substrate is then given as a sum of the individual contributions ΔE_k^{\pm} over the total number of phonon modes.

The complete dynamical simulation is worked out through three main steps:

- 1) A three-dimensional crystal is built up and the corresponding phonon frequencies and eigenvectors are computed.
- 2) A reasonable interaction potential for the O/O₂-silica system is assumed.
- 3) The dynamics is carried out solving self-consistently the Hamilton's equations of motion of the two oxygen atoms [Eq. (4)] and the dynamics of the phonons, i.e., by computing the phonon excitation strengths given in Eq. (9) at each time step of the classical trajectory.

It is worthwhile to notice that according to our collisional model, the reaction is adiabatic, so that the chemical species evolve in their ground electronic state while only the rotational and vibrational internal states can be excited. In model calculations performed by Swaminathan et al.,¹⁸ on the inelastic scattering of O from a silicon-like surface, it has been shown that the surface could also promote electronic transitions in the incoming oxygen atom. The opening of the electronic channel in addition to the molecular nuclear motions would drastically

increase the complexity of the chemical dynamics, and it has not yet been explored for surface recombination reactions.

III. Silica Structure and Lattice Dynamics

The β cristobalite is the silica phase that can exist at the temperatures involved in the re-entry conditions, i.e., is the surface temperature range between 600 and 2000 K.^{19,20} We have, therefore, built up a three-dimensional crystal lattice starting from the known arrangement of the silicon and oxygen atoms in the lattice bulk,²¹ such that the stoichiometry and the net neutrality of the crystal is fulfilled. Contrary to the case of the bulk structure, the atom arrangement on the top-most layer is problematic because as a result of the molecular character of silica, the surface structure cannot be uniquely determined. Recently, some structural properties of vitreous silica have been elucidated in molecular dynamic simulations, and the existence of a complex reconstructed surface layer with structural defects has been demonstrated.²² To overcome these structural problems, two different surfaces have been constructed and considered in the scattering calculations. This allows us to explore an interesting aspect in heterogeneous catalysis, i.e., the influence of the surface structure modifications on the catalytic activity of the substrate.

Surface A consists of 162 atoms disposed on 11 layers with the silicon atoms in the bulk and on the topmost layer bonded to four oxygen atoms according to the tetrahedral arrangement. This model surface would simulate a silica surface covered by oxygen atoms bonded to the underlining silicon atoms. Surface B consists of 149 atoms and it has been built up assuming bare silicon atoms with dangling bonds on the topmost layer. This second surface corresponds to a silica surface with the silicon sites unoccupied, and it is similar to the surface model assumed in the kinetic study by Jumper and Seward⁶ and Nasuti et al.⁷

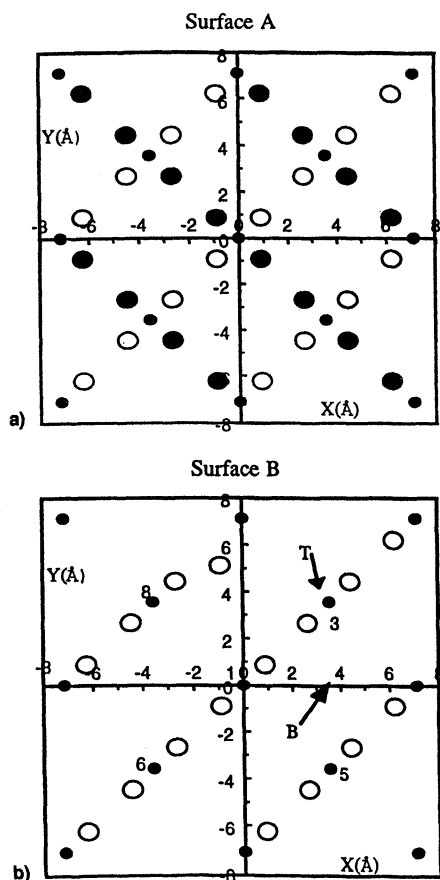


Fig. 1 a) X-Y projection of the first three layers for silica surface A. ●, first layer O atoms; ●, second layer silicon atom; ○, third layer O atom. b) As for Fig. 1a, but for surface B: ●, first layer silicon atom; and ○, second layer O atom. The T and B sites are shown.

Figure 1 shows the geometrical atom arrangement of the first uppermost layers for both surfaces.

The phonon frequency distribution and eigenvectors for the two surfaces are calculated by numerical diagonalization of the force constant dynamical matrix for the two crystals. The interaction potential of the atoms in the crystal matrix, given as the sum of two-body Si-O and O-O interactions, is given in Ref. 23, and it is constructed by adding the short-range Born-Mayer-Huggins forces to the long-range screened coulomb forces between the nearest and the next-nearest neighbor atoms. The potential parameters are given in Ref. 23.

The obtained phonon frequency distributions are shown in Fig. 2. The full frequency spectra for surfaces A and B are in good qualitative agreement with the vibrational spectrum reported in Ref. 24. In particular, the two sharp peaks appearing at about 640 cm^{-1} and at the highest frequency are well reproduced, whereas the relative intensity of the first maximum in the bulk spectrum ($\sim 400 \text{ cm}^{-1}$) is not reproduced. However, because the lattice Hamiltonian as well as the lattice dynamic model assumed in Ref. 24 and in the present work are different, we do not expect the spectra to agree completely. The frequency distributions for surfaces A and B are very similar

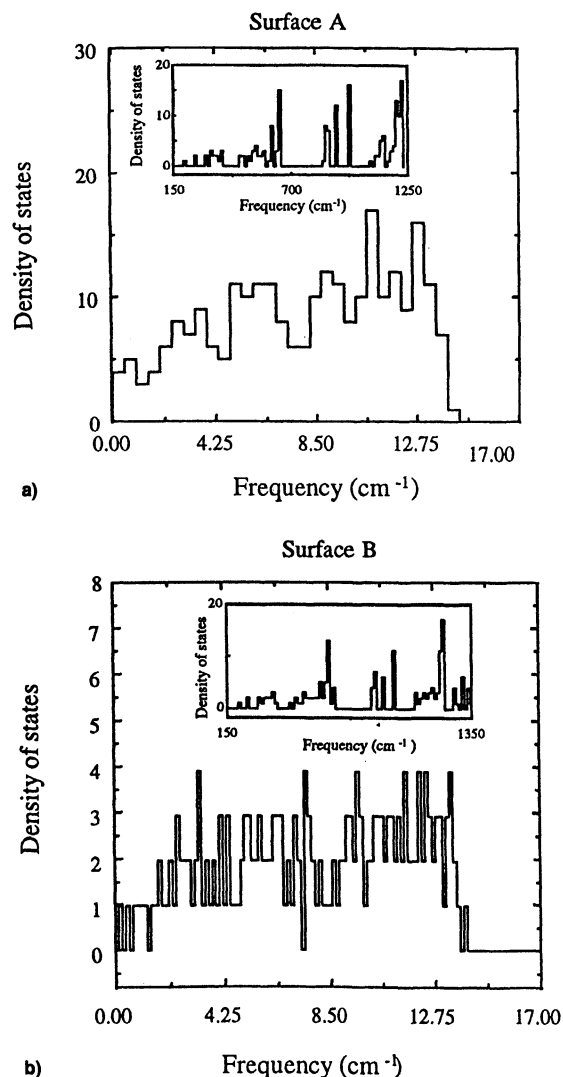


Fig. 2 a) Phonon frequency distribution of β cristobalite calculated from surface A consisting of 162 atoms disposed on 11 layers in the sequence O/16-Si/13-O/16-Si/8-O/22-Si/12-O/22-Si/8-O/16-Si/13-O/16 (in the insert the high-frequency distribution is shown). b) Phonon frequency distribution for surface B consisting of 149 atoms disposed on 10 layers in the sequence Si/13-O/19-Si/8-O/22-Si/12-O/22-Si/8-O/16-Si/13-O/16.

in the bulk region, although surface A exhibits a higher density of states in the low-frequency region. Because this frequency range associated with the surface phonon modes plays a larger role in the reaction dynamics, the different distributions observed in this region should have some consequences in controlling the catalytic activity of the two surfaces. It should be noted that, because the force field of the crystal is the same for both surfaces, the corresponding phonon spectra are obtained within the same accuracy.

IV. O₂-Silica Interaction Potential

In the case of molecular dynamic calculations, the search for an accurate potential energy surface, where the collision takes place, is always the most critical step. Because of the complete absence of ab initio calculations, as well as the lack of experimental information on the spectroscopic properties of the adsorbed atomic and molecular oxygen, the interaction potential for the O/O₂-silica system can only be tentatively constructed on a semiempirical ground. Therefore, from the known O-O interaction in the gas phase²³ and Si-O interactions in the lattice,²³ we have attempted the following interaction potential:

$$V_{\text{int}} = \sum_{j=1}^2 \sum_{m=1}^{N_1} A_{\text{Si-O}} \exp(-r_{mj}\rho^{-1}) + \sum_{j=1}^2 \sum_{n=1}^{N_2} \beta_{\text{O-O}} \exp(-\gamma r_{nj}) + V_c \quad (11)$$

where the first and the second term are the Si-O_{gas} and O-O_{gas} potential interactions, respectively, and r_{lj} is the distance between the l th and j th atom. The last term is the coulomb interaction between the quadrupole charge of the oxygen molecule and the charge on the silicon and oxygen lattice atoms:

$$V_c = \sum_{j=1}^2 \sum_{n=1}^N \frac{\delta_{\pm} Z_n e^2}{r_{nj}} \quad (12)$$

with $\delta_- = -0.958 \exp(-1.33R_{\text{O-O}})$ and $\delta_+ = 2\delta_-$, $R_{\text{O-O}}$ is the intramolecular distance in O₂. The potential parameters are given next: (energies are given in eV and lengths in Å), $A_{\text{Si-O}} = 1850$, $\rho = 0.29$, $\beta_{\text{O-O}} = 2.55$, and $\gamma = 4$. The potential surface obtained is obviously very uncertain. Nevertheless, on the basis of the rather good agreement between the experimental and calculated recombination coefficient, we claim that the general features of the recombination process can be reasonably described at a qualitative level with the potential assumed.

V. Trajectory Calculations

A. E-R Recombination Reaction

In the scattering calculations, the rate-determining step of Eq. (2) in the E-R reaction scheme is simulated. The oxygen atom in the gas phase strikes the surface at a given kinetic energy, E_{kin} , and initial polar angles $(\theta, \phi) = (0, 0)$. For each impact energy, the initial position coordinates of the gas-phase atom are randomly selected such that the aiming area covers uniformly the surface unit cell. Because one of the main objectives of this work is to investigate the influence played by the surface adsorption site on the recombination reaction, we explore the reaction dynamics assuming different sites for the adsorbed oxygen atom. Therefore, we have carried out three sets of calculations corresponding to the following different adsorption conditions:

- a) O_{ad} is randomly adsorbed within the surface unit cell.

- b) O_{ad} is bonded in the bridge site *B* (see Fig. 1).

- c) O_{ad} is adsorbed on the top of a silicon atom (site *T* in Fig. 1).

We assume that the adsorbed oxygen is in thermal equilibrium with the solid substrate, so that the normal component of the initial momentum P_z is set equal to KT_s . For each impact energy of the gas-phase oxygen we have computed a bunch of more than 1600 trajectories for the case studied a and around 400 trajectories for cases b and c. For each trajectory and at each collisional time step we monitored the total energy, the momenta and atom coordinates, the energy exchanged with the surface, and the rotational and vibrational energy of the formed O₂ molecule.

1. Case Studied (a)

Figure 3 shows the recombination probability $P_{\text{E-R}}(E_{\text{kin}})$ for the recombination reaction, $\text{O} + \text{O}_{\text{ad}} \times \text{silica} \rightarrow [\text{O}_2(v, j)]_{\text{gas}} + \text{silica}$, as a function of the kinetic energy of the oxygen gas atom in a wide range of impact energies from 0.001 to 3.8 eV. Within the limits of the semiempirical potential energy assumed in the calculations, the expected numerical accuracy of the calculated reaction probabilities is about 20%. As expected, because of the low catalytic activity of silica, the recombination probability is small. From Fig. 3, it can be noticed that the reaction probability has a maximum around $E_{\text{kin}} = 0.008$ eV, whereas beyond $E_{\text{kin}} = 0.003$ eV, $P_{\text{E-R}}$ rapidly decreases to zero.

Assuming that a flux of oxygen atoms hits the surface with a Maxwellian energy distribution, the recombination coefficient $\gamma(T_s)$ can be obtained by averaging the calculated recombination probabilities $P_{\text{E-R}}(E_{\text{kin}})$ over a Maxwell distribution at a given temperature. Thus, we get $\gamma = 0.029$ at $T_{\text{gas}} = T_s = 1000$ K. This semiclassical value can be considered in satisfactory agreement with the experimental $\gamma_{\text{exp}} = 0.0123$ reported by Greaves and Linnert⁵ at $T_s = 893$ K, considering that any fitting procedure of the potential parameters has been attempted. Nevertheless, it should be noted that the recombination coefficient given in Ref. 5 has been determined indirectly in reactor cell, that is, under conditions that are quite different from those simulated here, where a single particle collides with a well-defined, single-crystal silica surface. Therefore, the comparison between the experimental and the theoretical γ value, although of some interest, cannot be considered as persuasive as it appears.

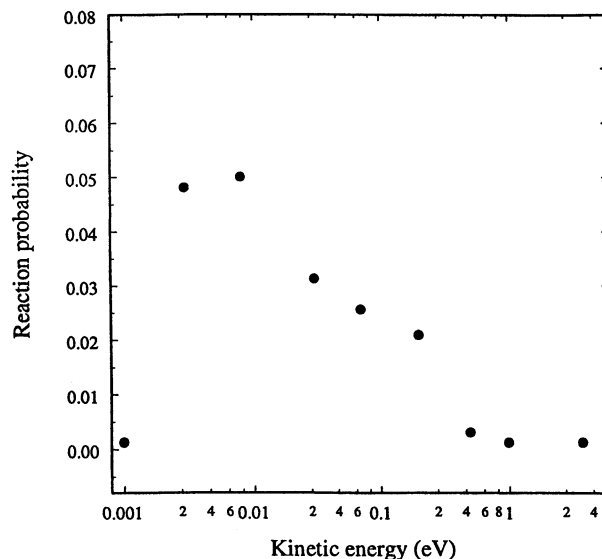


Fig. 3 E-R recombination probability for the process: $\text{O} + \text{O}_{\text{ad}} \times \text{silica} \rightarrow \text{O}_2(v) + \text{silica}$. O_{ad} is adsorbed within the unitary cell of the silica surface B. $T_s = 1000$ K.

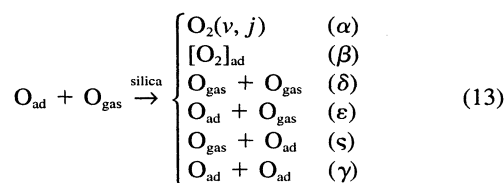
[§]Van der Avoird, private communication, Inst. of Theoretical Chemistry, Univ. of Nijmegen, ED Nijmegen, The Netherlands.

Table 1 Probabilities for the E–R reaction channels at different kinetic energies E_{kin} of the gas-phase oxygen atom^a

E_{kin} , eV	Channels					
	α	β	δ	ε	ς	γ
0.001	0.00	6.00(–2) ^b	4.50(–1)	5.14(–1)	0.00	0.00
0.003	4.81(–2)	1.60(–1)	4.87(–1)	2.77(–1)	1.56(–2)	1.25(–2)
0.008	5.00(–2)	8.10(–3)	7.97(–1)	1.41(–1)	0.00	0.00
0.03	3.13(–2)	0.00	8.30(–1)	8.3(–3)	1.28(–1)	0.00
0.07	2.56(–2)	0.00	6.90(–1)	2.38(–2)	2.59(–1)	1.36(–3)
0.20	2.13(–2)	0.00	4.03(–1)	6.63(–2)	4.88(–1)	2.19(–2)
0.5	3.13(–3)	1.00(–3)	2.85(–1)	8.50(–2)	5.35(–1)	9.20(–2)
1.0	1.25(–3)	1.88(–3)	2.81(–1)	9.91(–2)	5.00(–1)	1.17(–1)
3.8	1.25(–3)	1.50(–2)	6.38(–2)	6.00(–2)	4.76(–1)	3.84(–1)

^aAd-atom is adsorbed within the silica unit cell of surface B. $T_s = 1000$ K.^b6.00(–2) = 6.00×10^{-2} .

The interaction of the oxygen atoms with silica can lead to the activation of several surface processes that have been considered in the trajectory analysis:



The probabilities of the collisional events leading to processes (α – γ) are reported in Table 1.

The results obtained show that in the low-energy regime, there is a large probability for both the incoming and the adsorbed atom to be reflected from the surface into the gas phase. The probability for the O_2 formation in the gas phase is also substantial at low-impact energies, whereas the O_2 formation is practically prevented at energies higher than 3.8 eV. The fast decreasing of the E–R probability is caused by the increasing importance of the other reaction channels, in particular to the opening of channel (γ), where both the oxygen atoms are adsorbed after surface migration. In the high-energy collisional regime, there is, in fact, a marked tendency for the oxygen to be trapped, rather than to react and possibly desorb. This is an interesting result that could be of some relevance for the surface damage problems in shuttle re-entry conditions. The adsorption of atoms and molecules has two important consequences: firstly, a large amount of energy is released to the surface as a consequence of the strong coupling with the phonons; and secondly, the surface can be reconstructed because of the surface heating and the formation of the oxygen ad-layer. The analysis of the trajectories leading to O_{ad} and $[\text{O}_2]_{\text{ad}}$ shows that both effects are quite efficient on β cristobalite. Typically, O_{ad} and $[\text{O}_2]_{\text{ad}}$ are formed at collisional times of $\sim 25\tau$ ($\tau = 1.0 \times 10^{-14}$ s). The motion of the adsorbed atom/molecule takes place at distances from the surface plane no greater than 2.5 Å. Unfortunately, the migration of these species on the surface cannot be followed for times longer than 120τ because such strongly perturbed motion becomes rapidly unstable. Therefore, we cannot exclude that on a longer time scale the adsorbed oxygen atoms recombine as $[\text{O}_2]_{\text{gas}}$, nor that the $[\text{O}_2]_{\text{ad}}$ molecules finally desorb in the gas phase.

The energy partitioning among the internal states of the formed O_2 molecules and the vibrational motions of the lattice atoms is shown in Fig. 4, where the total energy fraction for vibrational (E_{vib}), rotational (E_{rot}), translational (E_{tr}), and the phonon excitation (ΔE_{ph}) for the recombination channel (α) is reported as a function of the kinetic energy of the gas-phase oxygen. The energy distribution is referred to as the final state of the free molecules, i.e., the motion of the O_2 molecule

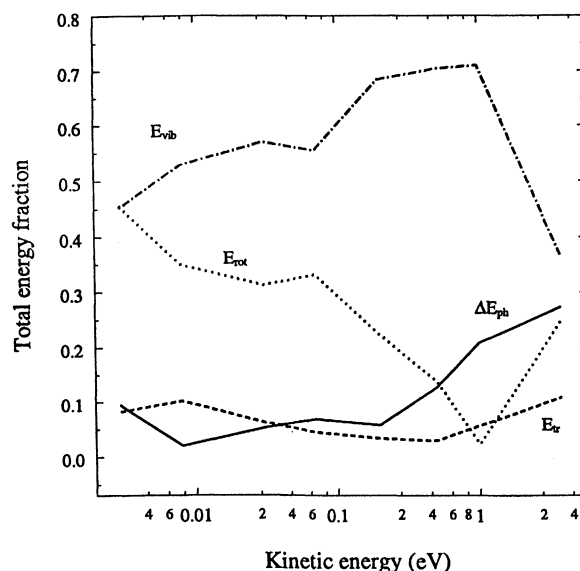


Fig. 4 Total energy partitioning in the E–R recombination process (α) as a function of the kinetic energy of the gas atom. Case study a for silica surface B.

formed at the surface and scattered off into the gas phase is followed far into the asymptotic region of the gas phase ($Z > 10$ Å).

From the obtained results, it is evident that the largest fraction of the reaction exothermicity goes into vibration, with a considerable rotational excitation apart from the lowest impact energy explored, where E_{vib} and E_{rot} are equivalent. In fact, the results show that the vibrational distributions are nonthermal with a large excitation probability of the medium-lying vibrational states. At higher collisional energies, the vibrational states with $v < 35$ are energetically accessible to the recombination dynamics. On the contrary, the energy loss to the surface is negligible, less than 10%, except at $E_{\text{kin}} = 1$ eV and $E_{\text{kin}} = 3.8$ eV. At these energies, almost 30% of the reaction exothermicity is transferred to the surface, whereas the energy available for vibrational excitation in O_2 is drastically reduced. Reliable considerations on energy partitioning at $E_{\text{kin}} = 1.0$ and 3.8 eV cannot be drawn, however, because of the very small reaction probability. The energy flow pathways shown in Fig. 4 are a consequence of the recombination mechanism through which the oxygen atoms recombine. From the trajectory analysis, it is shown that the reaction mechanism is mainly indirect: the adsorbed oxygen migrates on the surface before being scattered from the surface into the gas phase and finally reacting with the incoming gas atom. The O_2 molecules are formed in the gas phase at distances from the surface generally not

Table 2 Probabilities for the E-R reaction channels at different kinetic energies of the gas-phase oxygen atom^a

E _{kin} , eV	Channels					
	α	β	δ	ϵ	ς	γ
0.07	2.00(-2)	0.00	4.60(-1)	1.10(-1)	4.00(-1)	1.00(-2)
0.1	3.00(-2)	0.00	3.50(-1)	7.50(-2)	5.45(-1)	0.00
0.15	7.50(-3)	0.00	3.68(-1)	8.20(-2)	5.32(-1)	1.00(-2)
0.2	2.50(-2)	0.00	3.50(-1)	5.50(-2)	5.00(-1)	0.00
0.3	3.00(-2)	5.00(-3)	3.00(-1)	6.00(-2)	3.55(-1)	2.50(-1)
0.4	3.50(-2)	2.50(-2)	3.38(-1)	1.35(-1)	1.40(-1)	3.35(-1)
0.5	4.50(-2)	2.00(-2)	3.10(-1)	1.38(-1)	1.05(-1)	3.82(-1)
1.0	5.53(-2)	8.00(-2)	2.00(-1)	1.75(-1)	2.50(-2)	4.68(-1)
2.0	4.52(-2)	1.50(-1)	7.50(-2)	2.05(-1)	2.00(-2)	5.05(-1)
3.0	3.20(-2)	1.45(-1)	3.00(-2)	1.73(-1)	1.50(-2)	6.05(-1)
5.0	1.00(-2)	1.50(-1)	5.00(-3)	1.60(-1)	0.00	6.75(-1)

^aAd-atom is placed in site B of the silica surface B. $T_s = 1000$ K.

less than 3 Å. Under these conditions the coupling with the substrate is weak and only a small amount of the exothermicity is transferred to the surface.

2. Case Studied (b) and (c): Site and Surface Structure Effects

We now focus on the surface site effect on the recombination reaction. In Table 2, the recombination probabilities together with the probabilities for the other inelastic channels are reported at different impact energies of the gas atom while O_{ad} is adsorbed on surface site B in a bridge-like geometry.

The collision dynamics on this site is rather complex: virtually all of the inelastic channels are now energetically accessible. The inelastic channel (δ) is again very effective, but high probabilities are now observed for adsorption collisions with both oxygen atoms trapped at the surface. These collisional events are very frequent at the higher impact energies, the reason for this being the stronger coupling with the lattice atoms and the consequently high fraction of translational energy of the gas-phase oxygen converted into the vibrational motions of the lattice atoms.

The analysis of the inelastic trajectories shows that in many cases O_2 is formed as a collisional intermediate before dissociating into the final products. As an example, in Fig. 5, we have reported a typical trajectory for the process: $O + O_{ad} \times \text{silica} \rightarrow [O_2]_{ad} \times \text{silica} \rightarrow O + O_{ad} \times \text{silica}$, with O_{ad} initially adsorbed on surface site B. The Z distance from the surface plane of the two oxygen atoms [the top layer is in the (X-Y) plane], together with the interatomic distance of the two oxygen atoms as a function of the collisional time, is reported. We notice that O_2 is temporarily formed at the surface with a lifetime of $\sim 40\tau$.

The trajectory analysis shows that at the higher collisional energies there is a marked tendency for the temporarily formed O_2 molecules to be stabilized in a specific surface site through the opening of channel (β). Furthermore, the molecules are formed in highly vibrational and rotational excited levels, with a too-small residual translational energy for the molecules to be able to desorb in the gas phase. The probabilities reported in Table 2 for the adsorption processes β and γ should be taken with some precaution, however, because the final fate of these collisional events cannot be exactly known.

The energy partitioning for the recombination collisions is reported in Fig. 6, whereas in Fig. 7, the vibrational distribution of the nascent O_2 molecules detected at $E_{kin} = 1$ eV is shown. The influence of the surface structure modifications of the substrate on the recombination reaction is shown in Fig. 8, where we have reported the recombination probabilities assuming O_{ad} adsorbed on the site T of surfaces A and B. From this figure we notice that the presence of the oxygen ad-layer on surface A has an effect on the surface reactivity: the recombination probabilities for surface A are significantly higher than those observed for the clean surface B. The enhanced reactivity of site T with respect to site B is a result of its high specificity

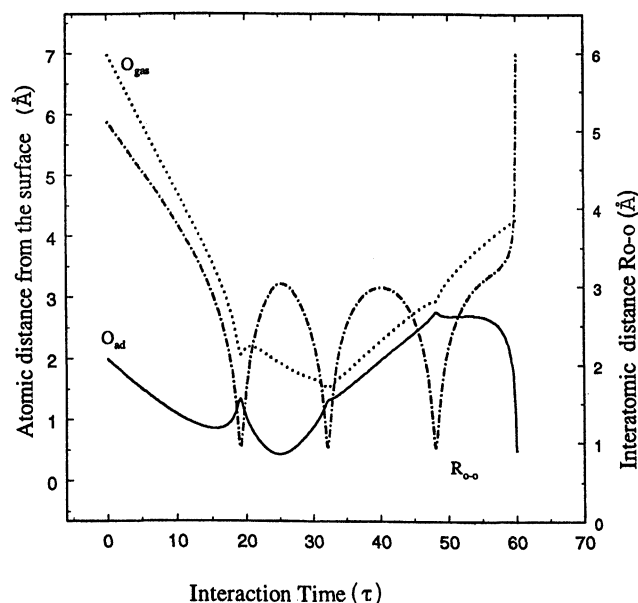


Fig. 5 Trajectories of two oxygen atoms for the process: $O + O_{ad} \times \text{silica} \rightarrow [O_2]_{ad} \times \text{silica} \rightarrow O + O_{ad} \times \text{silica}$, with O_{ad} initially adsorbed on surface site B. The Z distance from the surface for O_{ad} and O_{gas} is reported as a function of the interaction time. The intramolecular O-O distance (R_{O-O}) is also reported. The trajectory shows that O_2 is temporarily formed at the surface.

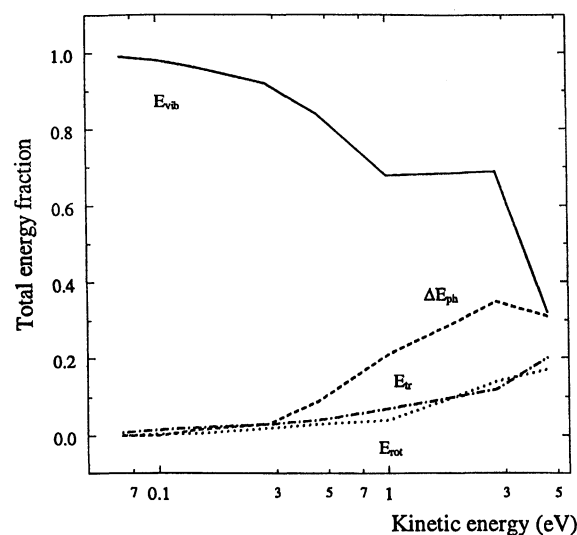


Fig. 6 Total energy distribution in the E-R recombination process (α): $O + O_{ad} \times \text{silica} \rightarrow O_2(v, j) + \text{silica}$. Case study b for silica surface B.

toward the interaction dynamics. The trajectory results show that practically only two channels are open to the site dynamics, i.e., the recombination reaction (α) and channel (δ), where both the oxygens are backscattered into the gas phase.

B. L-H-Type Recombination

According to the L-H recombination process, the reaction occurs between two adsorbed atoms, and because of that, this mechanism is expected to be in competition with the E-R mechanism under conditions of high surface coverage and for relatively low surface temperatures. At $T_s = 1000$ K, the L-H mechanism should be of minor importance with a predominant role played by the E-R recombination reaction. To assess the relative importance of the two mechanisms, we have made an attempt to simulate the L-H reaction. As for the E-R mechanism, we have assumed the following facts for the two adsorbed atoms' different site configurations:

- The two oxygen atoms are adsorbed randomly within the unitary cell of silica.
- One oxygen is placed on the top of the silicon atom 1, while the other is on silicon atom 3 (see Fig. 1).
- One oxygen is placed on top of silicon atom 1 while the other oxygen is placed on site B.
- The two oxygens are placed midway between silicon atoms 1 and 6 and silicon atoms 1 and 5, respectively.

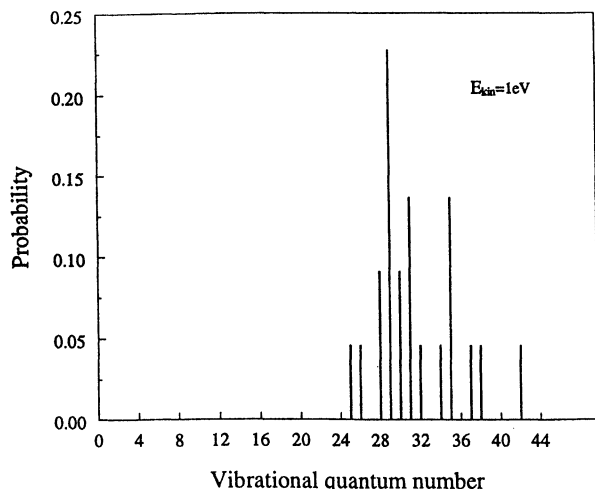


Fig. 7 Vibrational energy distribution at $E_{\text{kin}} = 1.0$ eV for the E-R recombination process (α): $\text{O} + \text{O}_{\text{ad}} \times \text{silica} \rightarrow \text{O}_2(v, j) + \text{silica}$. O_{ad} is placed in the B site.

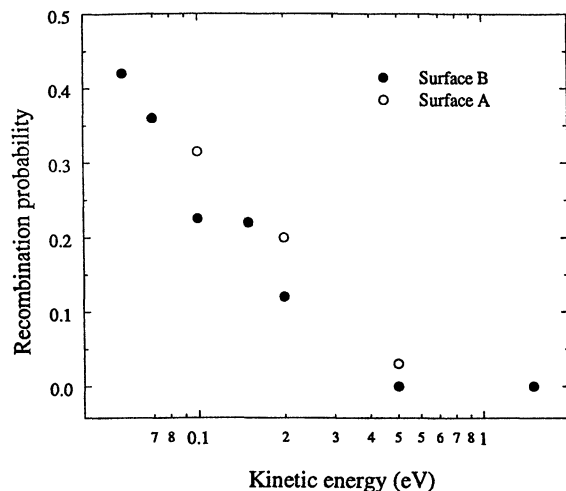


Fig. 8 Recombination probabilities for the process: $\text{O} + \text{O}_{\text{ad}} \times \text{silica} \rightarrow \text{O}_2(v, j) + \text{silica}$. O_{ad} is adsorbed on the T site of silica surface A and B.

For cases b-d, the initial position coordinates of both atoms are assumed randomly distributed within a restricted aiming area of 1 \AA^2 centered on the two sites and selected such that the interatomic O-O distance cannot be smaller than the asymptotic distance for free O_2 , i.e., $R_{\text{O-O}} \sim 3.5 \text{ \AA}$. The two oxygen atoms are thermally equilibrated with the surface, so that, as with the E-R simulation, the average Z component of the initial momenta is set equal to the surface temperature. Two-thousand trajectories have been run out for case 1, while 400 trajectories have been integrated for cases 2-4.

In Table 3, we reported the L-H recombination probabilities for the cases considered in the dynamical simulation. The total energy distribution among the internal states of the formed O_2 molecules and the substrate is also reported. As expected, at $T_s = 1000$ K the L-H recombination probability for case a is

Table 3 P_r and energy partitioning according to the L-H-like mechanism for case studied (a-d)^a

Case studied	P_r	E_{vib}	E_{rot}	E_{tr}	E_{ph}
a	2.30(-3)	59.0	23.1	10.2	7.7
b	3.85(-2)	19.2	5.3	45.0	30.5
	0.11 ^b	8.5 ^b	4.0 ^b	31.9 ^b	55.6 ^b
c	0.0	—	—	—	—
d	0.0	—	—	—	—

^a Total energy fraction (%) transferred to the molecular motions and the surface phonons is reported. $T_s = 1000$ K.

^b Values on this line refer to the silica surface A.

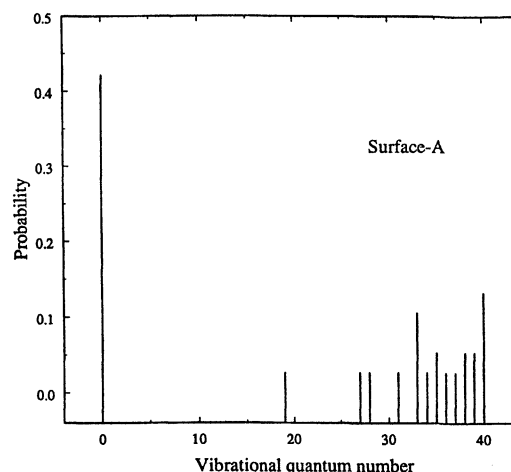


Fig. 9 Vibrational state distribution of the formed O_2 molecules in the L-H recombination reaction for surface A.

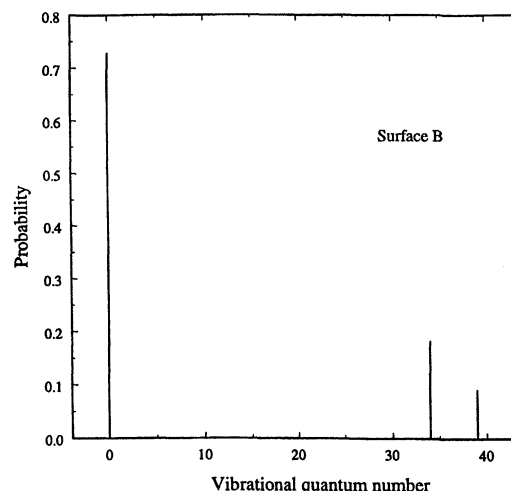


Fig. 10 As for Fig. 9, but for surface B.

Table 4 Theoretical and experimental recombination coefficients for oxygen atom recombination on silica surfaces

T_s , K	$\gamma(\text{E-R})$	$\gamma(\text{L-H})$	$\gamma(\text{exp.})$
600	0.033 ^a	0.0046 ^a	0.003
1000	0.029 ^a	0.0023 ^a	0.0123 ^b

^aSurface B. ^b $T_s = 893$ K.

smaller than the corresponding E-R probability by a factor close to 10. The energetics of the recombination reaction shows that the energy loss to the surface phonons is still a small fraction for reactive trajectories, whereas the largest fraction of the excess reaction exothermicity goes into the molecular vibrations for both mechanisms. The adsorption sites considered in the b geometry are very active for promoting the L-H reaction, whereas the sites considered under cases c and d are practically inert with zero recombination probability.

To show the influence of the oxygen ad-layer on the surface, for case b we have run the same trajectories on surface A and on surface B. The results reported in Table 3 show that the recombination probability on surface A is higher by a factor close to 3. The energy flows on surfaces A and B are different, although in both cases the oxygen molecules are mainly formed in the ground vibrational level (Figs. 9 and 10).

An interesting behavior that was expected from the L-H mechanism is the surface temperature effect on the recombination dynamics. From our results, we get at $T_s = 600$ K a recombination probability that is a factor of almost 2 greater than the probability at $T_s = 1000$ K. Because the surface coverage in the simulation is the same for both temperatures, the activation of the L-H reaction at the lower T_s is a result of the different dynamical coupling between the oxygen atoms and the surface phonons. No surface temperature effect has been observed for the E-R reaction mechanism: the same E-R trajectories calculated at $T_s = 1000$ and 600 K give exactly the same recombination probability. It is worthwhile to notice that, at $T_s = 600$ K, the calculated L-H recombination probability ($\gamma = 0.0046$) is in good agreement with the experimental value ($\gamma_{\text{exp}} \approx 0.003$) interpolated from the data reported in Ref. 5.

For the sake of clarity, in Table 4 we show the theoretical recombination coefficients for the E-R and L-H recombination reactions on the silica surface B, together with the corresponding experimental values at the two extreme surface temperatures considered in this work.

A comparison between the calculated and experimental γ values would confirm the switching of the reaction mechanism from E-R to L-H in the same manner as decreasing the surface temperature. Obviously, the crossover from the E-R to the L-H mechanism would require more calculations, and a consequently prohibitive computational time demand, at intermediate temperatures.

VI. Conclusions

Several interesting aspects concerning the recombination dynamics of the oxygen atoms on a silica surface have emerged in this work. We have found that, at $T_s = 1000$ K, the formation of O_2 molecules catalyzed by β -cristobalite occurs via an indirect E-R-type mechanism, according to which the reaction takes place through a surface migration of the adsorbed oxygen followed by recombination in the gas phase at distances from the surface larger than 3.5 Å. The L-H probability at this temperature is a factor of 10 smaller than the E-R probability. A direct consequence of the observed E-R mechanism is that the O_2 molecules are formed in highly vibrationally and rotationally excited states, whereas only a negligible fraction of the reaction exothermicity is transferred as heat to the surface (contrary to what is generally assumed in kinetic modeling). In fact, we found that the processes most likely causing surface damage are the adsorption processes. As the kinetic energy of

the impinging atom increases, the surface exhibits a marked tendency to trap both oxygens as O_2 or as atoms, resulting in huge energy transferred to the surface vibrations. The E-R γ coefficient at $T_s = 1000$ K is in satisfactory agreement with the experimental value reported by Greaves and Linnett.⁵ Nevertheless, our surface does not support any temperature effect on the E-R probability. Such an effect is found for the L-H probability. Our calculations indicate that the L-H probability increases by a factor 2 as T_s decreases from 1000 to 600 K. The L-H probability is, at $T_s = 600$ K, in good agreement with the experimental findings. The effects of the adsorption site and atom arrangements on the top surface layer have also been explored in this work. Both effects have a large impact on the recombination probability, indicating that surface structure modification (or surface coverage) would significantly change the catalytic activity of the silica substrate. The results obtained in this work are obviously a consequence of the potential energy surface assumed in the calculations. This potential has been obtained on a semiempirical basis, and it must be regarded as a crude approximation to the real (unknown) interaction forces. Therefore, the reported results should be taken with some precaution, although the satisfactory agreement between the theoretical and the experimental γ values would suggest that the general features of the recombination dynamics are correctly described within the framework of these simulations.

Acknowledgments

This research is supported by the Italian Space Agency. The authors are grateful to P. De Felice for her contribution in the early stages of this work, and to C. Bruno for fruitful discussions.

References

- Scott, C. D., "Effect of Nonequilibrium and Catalysis on Shuttle Heat Transfer," AIAA Paper 83-1485, June 1983.
- Gousset, G., Panafieu, P., Touzeau, M., and Vialle, M., "Experimental Study of a D.C. Oxygen Glow Discharge by V.U.V. Absorption Spectroscopy," *Plasma Chemistry and Plasma Processes*, Vol. 7, No. 4, 1987, pp. 409-427.
- Markovic, V. L., Petrovic, Z. L., and Pejovic, M. M., "Surface Recombination of Atoms in a Nitrogen Afterglow," *Journal of Chemical Physics*, Vol. 100, No. 11, 1994, pp. 8514-8521.
- Berkut, V. D., Doroshenko, V. M., Kovtun, V. V., Koudryavtsev, N. N., Novikov, S. S., Smirnov, N. V., and Sharotovov, A. I., "Measurements of the Probability of the Heterogeneous Atom Recombination on Heated Surfaces in a Supersonic Flow," *Soviet Journal of Chemical Physics*, Vol. 9, 1992, pp. 2222-2237.
- Greaves, J. C., and Linnett, J. W., "Recombination of Atoms at Surfaces, Part 6—Recombination of Oxygen Atoms on Silica from 20°C to 600°C," *Transactions of the Faraday Society*, Vol. 55, 1959-II, pp. 1355-1361.
- Jumper, E. J., and Seward, W. A., "Model for Oxygen Recombination on Reaction-Cured Glass," *Journal of Thermophysics and Heat Transfer*, Vol. 8, No. 3, 1994, pp. 460-465.
- Nasuti, F., Barbato, M., and Bruno, C., "Material-Dependent Catalytic Recombination Modeling for Hypersonic Flows," *Journal of Thermophysics and Heat Transfer*, Vol. 10, No. 1, 1996, pp. 131-136.
- Gordietz, B., Ferreira, C. M., Nahorny, J., Pagnon, D., Touzeau, M., and Vialle, M., "Surface Kinetics of N and O Atoms in $\text{N}_2\text{-O}_2$ Discharges," *Journal of Physics D: Applied Physics*, Vol. 29, No. 4, 1996, pp. 1021-1031.
- Billing, G. D., and Cacciatore, M., "Semiclassical Calculation on the Probability for Formation of CO_2 on a Pt(111) Surface," *Chemical Physics*, Vol. 103, 1986, pp. 137-150.
- Billing, G. D., and Cacciatore, M., "Semiclassical Calculation of the Reaction Probability for the Process: $\text{C} + \text{O} \rightarrow \text{CO}$ on a Pt(111) Surface," *Chemical Physics Letters*, Vol. 113, No. 1, 1985, pp. 23-28.
- Tully, J. C., "Dynamics of Gas-Surface Interactions: Reaction of Atomic Oxygen with Adsorbed Carbon on Platinum," *Journal of Chemical Physics*, Vol. 73, No. 12, 1980, pp. 6333-6342.
- McCreery, J. H., and Walken, G., Jr., "Atomic Recombination Dynamics on a Solid Surface: $\text{H}_2 + \text{W}(001)$," *Journal of Chemical Physics*, Vol. 64, No. 7, 1976, pp. 2845-2853.
- Jackson, B., and Persson, M., "A Quantum Mechanical Study of

Recombinative Desorption of Atomic Hydrogen on a Metal Surface," *Journal of Chemical Physics*, Vol. 96, No. 3, 1992, pp. 2378–2386.

¹⁴Cacciatore, M., and Billing, G. D., "Dynamical Relaxation of $H_2(v, j)$ on a Copper Surface," *Surface Science*, Vol. 232, 1990, pp. 35–50.

¹⁵Cacciatore, M., and Billing, G. D., "Dissociation and Atom Recombination of H_2 and D_2 on Metallic Surfaces: a Theoretical Survey," *Pure and Applied Chemistry*, Vol. 28, No. 5, 1996, pp. 1075–1081.

¹⁶Billing, G. D., and Cacciatore, M., "A Semiclassical Multi-Dimensional Study on the Inelastic and Reactive Interaction of $D_2(v, j)$ with a Non-Rigid Cu(111) Surface," *Faraday Discussions*, No. 96, 1993, pp. 33–42.

¹⁷Billing, G. D., "The Dynamics of Molecule-Surface Interactions," *Computational Physics Report*, Vol. 12, No. 6, 1990, pp. 383–450.

¹⁸Swaminathan, P. K., Garrett, B. C., and Murthy, C. S., "Electronic Excitation and Quenching of Atoms at Insulator Surfaces," *Journal*

of Chemical Physics, Vol. 88, No. 4, 1988, pp. 2822–2830.

¹⁹Wells, F. A., *Structural Inorganic Chemistry*, 4th ed., Clarendon, Oxford, England, UK, 1975, pp. 803–806.

²⁰*Engineering Property Data on Selected Ceramics*, Vol. III, Single Oxide MCIC-HB-07, Metals and Ceramics Information Center, Columbus, OH, July 1981.

²¹Wickoff, R. W. G., "The Crystal Structure of the High Temperature Form of Cristobalite (SiO_2)," *American Journal of Science*, Vol. 5, No. 9, 1925, pp. 448–459.

²²Feuston, B. P., and Garofalini, S. H., "Topological and Bonding Defects in Vitreous Silica Surface," *Journal of Chemical Physics*, Vol. 91, No. 1, 1989, pp. 564–570.

²³Feuston, B. P., and Garofalini, S. H., "Empirical Three-Body Potential for Vitreous Silica," *Journal of Chemical Physics*, Vol. 89, No. 9, 1988, pp. 5818–5824.

²⁴Sen, P. N., and Thorpe, M. F., "Phonons in AX_2 Glasses: from Molecular to Band-like Modes," *Physical Review B*, Vol. 15, No. 8, 1977, pp. 4030–4038.

AIAA DISPATCH

Focusing on

scientific

and technical

information,

AIAA Dispatch

can deliver what

you need, when

you need it.

TAP INTO:

- journal articles
- book chapters
- technical reports
- specifications and standards
- conference papers
- tables of contents and indices
- government documents
- patents

24-hour turnaround*

Quick, cost-effective, and easy to use

*Order fulfillment or notification of status within 24 hours provided request is correctly cited and in scope.

The aerospace community's premiere
DOCUMENT DELIVERY SERVICE

FEATURING MORE THAN

2 MILLION

REFERENCES.

For more information
or
to place an order:

- Call us at
800/662-1545
or
816/363-4600
- Fax us at
816/926-8794
- Send us an e-mail
message at
dispatch@lhl.lib.mo.us
- Visit the Linda Hall
Web site at
<http://www.lhl.lib.mo.us>

**AEROSPACE
ACCESS**
INFORMATION SERVICES FROM AIAA

AMERICAN INSTITUTE OF
AERONAUTICS AND ASTRONAUTICS
in cooperation with the Linda Hall Library.

AIAA

98-090